ISSN 1063-7761, Journal of Experimental and Theoretical Physics, 2011, Vol. 113, No. 6, pp. 1006–1014. © Pleiades Publishing, Inc., 2011.
Original Russian Text © V.E. Zobov, A.A. Lundin, 2011, published in Zhurnal Eksperimental'noi i Teoreticheskoi Fiziki, 2011, Vol. 140, No. 6, pp. 1150–1159.

ORDER, DISORDER, AND PHASE TRANSITION IN CONDENSED SYSTEM

Decay of Multispin Multiple-Quantum Coherent States in the NMR of a Solid and the Stabilization of Their Intensity Profile with Time

V. E. Zobov[a] and A. A. Lundin[b]

[a] *Kirensky Institute of Physics, Siberian Branch, Russian Academy of Sciences, Krasnoyarsk, 660036 Russia*
e-mail: rsa@iph.krasn.ru

[b] *Semenov Institute of Chemical Physics, Russian Academy of Sciences, Moscow, 117977 Russia*
e-mail: andylun@orc.ru

Received March 24, 2011

Abstract—Variations, experimentally observed in [14], in the intensity profiles of multiple-quantum (MQ) coherences in the presence of two special types of perturbations are explained on the basis of the theory, earlier developed by the authors, of the growth of the effective size of correlated clusters (the number of correlated spins) and the relaxation of MQ coherent states [23]. The intensity and the character of perturbation were controlled by the experimenters. It is shown that the observed stabilization of profiles with time is not associated with the stabilization of the cluster size. Quite the contrary, a cluster of correlated spins monotonically grows, while the observed variations in the intensity profile and its stabilization with time are attributed to the dependence of the decay rate of an MQ coherence on its order (its position in the MQ spectrum). The results of the theory are in good agreement with the experimental data.

DOI: 10.1134/S1063776111140111

1. INTRODUCTION

The intensive development of experimental methods of multipulse NMR spectroscopy of condensed media has led to the formation of multiple-quantum (MQ) NMR spectroscopy [1]. The physics behind this spectroscopy is the transformation, by means of sequences of high-power rf pulses, of the original Hamiltonian of internuclear spin–spin interactions into a new Hamiltonian (spin alchemy) under which the original magnetization is transformed into different rather complicated multifrequency time correlation functions [1–4]. It is these functions that indicate the emergence of MQ states in the spin system.

The emerging coherences and their dynamics provide a powerful and often irreplaceable means to study the behavior of particles in different systems: their clusterization and the rise of local structures situated, for example, on surfaces, in liquid crystals, in nanosize voids, etc. [5–7]. Depending on the experimental program, MQ coherences may or, generally speaking, may not (see below) be subjected to different additional (for example, relaxational) effects. At the final stage of the experiment, a time reversal is performed by means of a magic sandwich, owing to which the order is again transferred to the magnetization [8, 9].

Even if we set aside the above-mentioned applied aspects of MQ NMR spectroscopy, which ensure its widest application (from superconductivity studies to medicine), to realize its fundamental value, it suffices to note that the methods of MQ spectroscopy allow for the experimental study of the development of multiparticle (multispin) correlations with time through the observation of emerging coherences by means of MQ NMR [10–17], which, of course, is essentially important for the statistical mechanics of irreversible processes [18].

The study of the rise and decay of multiparticle correlations is of primary importance for modern methods of processing quantum information and for quantum computations. When implementing these methods, one controls the coherences prepared in a nuclear spin system by sequences of rf pulses, thus initiating the required processes. Note that the practical application of the huge potential of quantum computers requires the careful control of a quantum register; the more qubits (spins) are contained in the system, the more careful this control should be, because, as the number of correlated spins increases, the instability (brittleness) of the arising clusters increases due to the development of various relaxation processes that destroy the quantum-mechanical superposition of states in the system.

Thus, one of the central (and also the most complicated) problems in the field of spin MQ dynamics is the problem of relaxation (degradation of coherence [19]) of an MQ register depending on time, its size, quantum number, and the imperfections of the pulse sequences applied. In [10–12, 14, 15], this dependence was investigated experimentally on protons in

an adamantane and on fluorine nuclei in CaF_2. The authors of [10–12, 15] analyzed the growth of coherences and their relaxation under either a secular part of the internuclear dipole–dipole interaction or the same interaction transformed by pulse sequences. In [14], the method was significantly modified for the first time. The declared aim of the modification was to analyze the question of how far quantum information can be transmitted in the presence of isolators of finite (and controlled by an experimenter) accuracy. In other words, the authors analyzed the question of how large size can a cluster of correlated spins (a quantum register) reach under these conditions. The authors of [14] observed the growth of clusters of correlated spins by introducing a controlled perturbation into the Hamiltonian that produces these clusters. They assumed that the maximum size of a cluster under these conditions is limited, and clusters of maximum size are in dynamic equilibrium with the environment: if the original size of a cluster is greater than its equilibrium value, then it decreases under a perturbing Hamiltonian, whereas the unperturbed Hamiltonian leads to an unlimited growth of the cluster size. According to the authors of [14], the size of the equilibrium cluster decreases as the perturbation intensity increases. As was assumed in [14], the process described above is the Anderson localization [20].

In [23], based on the adiabatic approximation (a modified Anderson model) [21, 22], we solved the problem of relaxation of MQ coherences by a conventional experimental scheme (Fig. 1a). In the present paper, based on the earlier developed growth theory of correlated clusters under ideal conditions [16] and the relaxation theory of MQ coherences [23], we explain the variations in the intensity profile of MQ coherences, observed in [14], and show that the stabilization of this profile with time is not associated with to the stabilization of the cluster size. Namely, the cluster of correlated spins monotonically grows, while the observed variations in the intensity profile (MQ spectrum) and its stabilization are determined by the dependence of the decay rate of an MQ coherence on its order (its position in the MQ spectrum).

In the next section, we consider the original nuclear spin system and a method for producing MQ coherences and give a brief summary of the main results obtained on the basis of a modified Anderson model [23], which are important for the further account. In Section 3, we study a variation in the bandwidth of an MQ spectrum in the situation when the decay of MQ coherences is due to the secular part of the dipole–dipole interaction, which serves as a "control" system on a separate distinguished time interval following the interval in which these MQ coherences were produced. In Section 4, we consider the variation of an MQ coherence profile when two processes are superposed on a single time interval: the creation of coherences and their degradation [14]. Finally, in Section 5, we discuss the results obtained and compare them with experimental data. In the Appendix, we evaluate in detail the formula for the second moment of the autocorrelation function, which determines the growth rate of the number of coherent states.

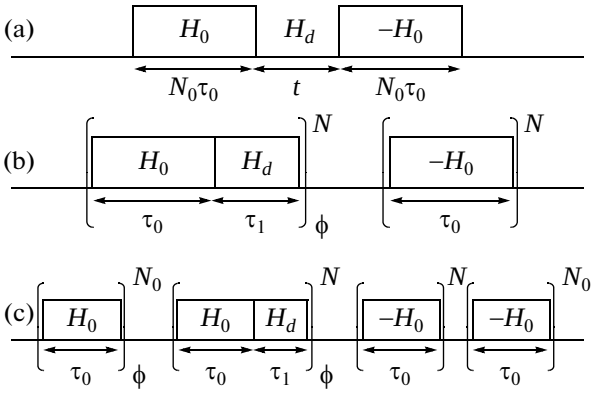

Fig. 1. (a) A standard scheme of experiment on the observation of MQ NMR. Interactions H_0, H_d, $-H_0$ determine the development of the spin system at appropriate stages. (b) The first of the experimental schemes implemented in [14]. The formation of MQ coherences for $\tau_1 = 0$ occurs without failures. (c) The second of the experimental schemes implemented in [14]. A cluster of given mean size is initially formed in the system during time $N_0\tau_0$; the development of this cluster is subsequently followed up.

2. DYNAMICS AND RELAXATION OF MQ COHERENCES IN A SOLID

It is well known [22] that the broadening of NMR lines in nonmetallic diamagnetic solids is mainly attributed to the secular part of internuclear dipole–dipole interactions, which completely determines the dynamics of a nuclear spin system:

$$H_d = \sum_{i \neq j} b_{ij} S_{zi} S_{zj} - \frac{1}{2} \sum_{i \neq j} b_{ij} S_{+i} S_{-j} \equiv H_{zz}^0 + H_{ff}, \quad (1)$$

where $b_{ij} = (1/2)\gamma^2\hbar(1 - 3\cos^2\theta_{ij})/r_{ij}^3$, $\mathbf{r}_{ij}$ is a vector connecting spins i and j, θ_{ij} is the angle between the vector $\mathbf{r}_{ij}$ and an external dc magnetic field, γ is the gyromagnetic ratio, and $S_{\alpha i}$ is the α-component ($\alpha = z, +, -$) of the vector operator of spin at site i. Henceforth, we express energy in frequency units.

When using pulse methods in the NMR of solids, the basic Hamiltonian (1) is usually transformed by spin alchemy (various sequences of rf pulses) into other Hamiltonians that are of interest for the researcher [24]. For example, in the conventional MQ

NMR spectroscopy, the original Hamiltonian is transformed into the effective Hamiltonian

$$H_0 = -\frac{1}{4}\sum_{i\neq j} b_{ij}(S_{+i}S_{+j} + S_{-i}S_{-j}), \quad (2)$$

which is nonsecular with respect to the external dc magnetic field. Under the effect of this Hamiltonian during the so-called preparation period of length τ_0, the original magnetization is transformed into various rather complicated time correlation functions that depend on the product of a various number of spin operators. Note that, because the preparation period in some experimental methods is isolated and is repeated a large number of times N_0 (Fig. 1), it is expedient to introduce an additional time $T_0 = N_0\tau_0$. Now, the equilibrium high-temperature density matrix in a strong static magnetic field $\mathcal{H}_0$ is represented as [22]

$$\rho_{eq} \propto 1 + \frac{\gamma\hbar\mathcal{H}_0}{kT}\sum_{j=1}^{N_S} S_{zj},$$

where k is the Boltzmann constant, T is temperature, and N_S is the total number of spins in a sample. This matrix is transformed into a nonequilibrium density matrix, which is conveniently represented as a sum ρ_M of off-diagonal elements with a certain difference of M magnetic quantum numbers, called MQ coherences (M is the order of a coherence, which simultaneously numbers the position of the coherence in the MQ spectrum),

$$\rho(t) = \exp(-iH_0t)\rho_{eq}\exp(iH_0t) = \sum_M \rho_M(t),$$
$$\rho_M(t) = \sum_{Q=M}^{Q=N_S}\sum_{\{i\}}\sum_q g_{QMq\{i\}}(t)|QMq\{i\}\rangle, \quad (3)$$

where $|QMq\{i\}\rangle$ is a basis operator in which Q one-spin operators form a product that relates Zeeman states differing by M units and $\{i\}$ are the numbers of sites of the crystalline lattice occupied by a given cluster. Thus, $\{i\}$ is in fact a multi-index. The summation over $\{i\}$ implies the summation over both the set of clusters and the set of spins in each cluster. The expression under the summation sign depends only on the differences of coordinates; i.e., the dependence on one of the coordinates is missing. Setting this coordinate to be arbitrary, we find that, with respect to other coordinates, the expression under summation decays quite rapidly. Thus, a cluster is a group of spins for which the expression under summation is not negligible. In (3), the index q numbers different basis states with identical values of Q and M. The coherences arising during the period T_0 are marked by a phase shift ϕ [2, 3]. The arising phase shift is proportional to $M\phi$, where M is an integer. Thus, Q-spin correlations are additionally distinguished by the number of quanta ($M \le Q$) [1–3]. Below, the amplitude of an M-quantum coherence can be separated as the Mth harmonic of an appropriate Fourier series.

Further, according to the conventional experimental scheme (Fig. 1a), these coherences are relaxed over a period of time t under the action of the secular dipole–dipole Hamiltonian (1). After the period of free evolution, a new sequence of pulses is applied to the system, that reverses the sign of the effective Hamiltonian (2); thus, a time reversal is performed [8, 9], owing to which the order again returns to the observed quantity—the single-quantum longitudinal magnetization. The amplitude of the partial (for a given value of M) magnetization can be measured by means of a $\pi/2$ pulse that turns the magnetization into the plane perpendicular to the external magnetic field. To determine the relaxation rate, one repeats the experiment many times for different values of t.

Following the simplest statistical model [2, 3], we assume in experiments that the distribution of coherences of different orders in the MQ spectrum is Gaussian:

$$g_M(N_0\tau_0) \propto \exp[-M^2/K(N_0\tau_0)].$$

The dispersion $K(N_0\tau_0)/2$ of distribution in this model is determined by the number $K(N_0\tau_0)$ of spins among which a dynamic correlation is established due to interaction (2) over the preparation time $T_0 = N_0\tau_0$. This number, called the number of correlated spins, or the effective cluster size, increases with the preparation time T_0.

In [14], the variation in the MQ coherence profile was studied by two variants of the modified method (Figs. 1b and 1c). According to the scheme of Fig. 1b, the authors of [14] combined, during the preparatory period, the effects of the Hamiltonian that produces MQ coherences (Hamiltonian (2)) and the Hamiltonian responsible for their relaxation (Hamiltonian (1)). Thus, the effective Hamiltonian in the preparatory period in the scheme of Fig. 1b is given by

$$H_{eff} = (1-p)H_0 + pH_d. \quad (4)$$

In this case, the time interval τ (duration of a cycle) of action of Hamiltonian (4) on the system is decomposed into two adjoined intervals: in the first interval, Hamiltonian (2) acts during time τ_0, and in the second, Hamiltonian (1) acts during time τ_1. The constant p in expression (4) is defined by the condition

$$p = \tau_1/\tau = \tau_1/(\tau_0 + \tau_1). \quad (5)$$

The second variant of the experiment carried out in [14] involved the sequence shown in Fig. 1c. In this approach, a cluster of a certain size was formed during a preparatrory period of full duration $N_0\tau_0$. This size was determined by the duration $N_0\tau_0$ of the interval. Then, during the interval $N\tau = N(\tau_0 + \tau_1)$, the system developed under Hamiltonian (4), which allowed one to trace the relaxation of the cluster of the given size after the time interval of $(N + N_0)\tau_0$ allotted for the mixing (recovery) of the system.

3. GROWTH AND DECAY OF MQ COHERENCES IN SEPARATE PROCESSES OF FORMATION AND DEGRADATION OF PHASE CORRELATIONS IN A SPIN SYSTEM

Just as in [23], we will consider an individual cluster from the sum in formula (3), that consists of Q spins, is situated in the set $\{i\}$ of sites of a crystalline lattice with fixed geometry, and has the coherence order M. Within the period of free evolution under interaction (1), the operator component of the density matrix is generally varied. These variations should obviously be accompanied by variations in the parameters Q, q, and $\{i\}$. The parameter M is preserved because Hamiltonian (1) commutes with the Zeeman operator. However, if the cluster is large enough, then, for not too large times, one can neglect variations in the dipolar energy and other numbers. Since the main role during the emergence and development of MQ coherences is played by phase correlations that arise and degrade in the spin system, here, just as in [23], it is expedient to apply a modified Anderson model (an adiabatic approximation). In accordance with this model, we will assume that only the phase of the operator component of the density matrix is varied:

$$\rho(M, Q, q, l, \{i\}|t) = |M, Q, q, l, \{i\}\rangle \times \exp\left[-i\int_0^t dt_1 \omega(M, Q, q, l, \{i\}|t_1)\right]. \quad (6)$$

Here l is the number of S_{zk} operators in the operator $|M, Q, q, l, \{i\}\rangle$. Then, according to the results of [23], for the conventional experimental method (Fig. 1a), the MQ coherence profile as a function of the order M and time is expressed as

$$g_M(N\tau_0, t) = \frac{2}{\sqrt{\pi K(N\tau_0)}}\exp\left(-\frac{M^2}{K(N\tau_0)}\right) \times \exp(-A^2M^2t^2)\exp\left(-\frac{K(N\tau_0)b^2t^2}{2}\right). \quad (7)$$

The constants A^2 and b^2 are directly related to the lattice sums of the coefficients b_{ij} of Hamiltonian (1). We should stress once again that, in equation (7), $K(N\tau_0)$ is the total number of correlated spins formed during time $N\tau_0$ under interaction (2) alone, that exhibits purely exponential growth [10, 11, 16].

In the experiments in [14], the authors determine the average effective size $K_{\text{eff}}(N\tau_0, t)$ of a cluster by the half-maximum bandwidth of the spectrum; therefore, it is expedient to introduce again the effective Gaussian distribution function that characterizes the intensity profile as a function of M:

$$\exp\left[-\left(\frac{1}{K(N\tau_0)} + A^2t^2\right)M^2\right] \times \exp\left[-\frac{K(N\tau_0)b^2t^2}{2}\right] = \exp\left[-\frac{M^2}{K_{\text{eff}}(N\tau_0)}\right]\exp\left[-\frac{K(N\tau_0)b^2t^2}{2}\right].$$

Now, the degradation of a cluster defined by time-dependent Gaussian multipliers in (7) can be taken into consideration as follows:

$$K_{\text{eff}}(N\tau_0, t) = \frac{1}{1/K(N\tau_0) + A^2t^2}. \quad (8)$$

The first and the last multipliers in (7) have no effect on the effective size of a cluster because they do not depend on the number M. The effect of these multipliers manifests itself in the variation of the amplitude of the entire spectrum. According to (8), the bandwidth of the MQ spectrum and the $K_{\text{eff}}(N\tau_0, t)$ decrease as the decay time increases (the evolution time with Hamiltonian (1)), which completely agrees with the experimental results of [12].

4. GROWTH AND DECAY OF MQ COHERENCES IN THE SIMULTANEOUS PROCESS OF FORMATION AND DEGRADATION OF PHASE CORRELATIONS IN A SPIN SYSTEM

Unlike conventional MQ experiments, the variations that were introduced in [14] (see Figs. 1b and 1c) lead to the substitution of a single Hamiltonian (4) for Hamiltonians (1) and (2) acting separately on different time intervals. As is shown below, these variations manifest themselves in the experiment, first, in the decrease of the growth rate of MQ coherences compared with the case of $p = 0$ and, second, in the appearance of additional decay different from that defined by (7).

Since a quantity that characterizes the number of spins between which a dynamic correlation is established during the preparatory period is given by the second moment of the MQ coherence intensity profile [16],

$$\langle\langle n^2(N\tau)\rangle\rangle_{\text{eff}} = K(N\tau),$$

we should next evaluate the variation in the time dependence of this second moment for $0 < p < 1$ compared with the result given by (8).

In [16], we developed an appropriate diagram technique to evaluate the above-mentioned second moment. Since the processes of the development and mixing of correlations in the experiment generally occur in different time intervals ($N\tau$ and $N\tau_0$), these processes were described by two independent propaga-

tors: $G(N\tau)$ and $G(N\tau_0)$, respectively (see formula (42) in [16]). Now, while the propagator $G(N\tau_0)$ with reversed time (with the Hamiltonian $-H_0$) at the stage of mixing remains unchanged, in the propagator $G_p(N\tau)$, which corresponds to the stage of development of correlations, one should replace H_0 by H_{eff} (4). Thus, the propagator $G_p(N\tau)$ is now represented as a series

$$G_p(N\tau) = \sum_{m=1}^{\infty} \omega_c^m \int_0^{N\tau} dt_1 \int_0^{t_1} dt_2 \ldots \int_0^{t_{m-1}} dt_m \times \Gamma_p(t-t_1)\ldots\Gamma_p(t_{m-1}-t_m)\Gamma_p(t_m), \quad (9)$$

containing the convolutions of one-spin autocorrelation functions, which were approximated in [16] by Gaussian functions with the averaged second moment:

$$M_{2c}(p) = \frac{5}{4}C^2(1-p)^2\left(1+2.4\frac{p^2}{(1-p)^2}\right) = M_{2c}(0)(1-p)^2\left(1+2.4\frac{p^2}{(1-p)^2}\right), \quad (10)$$

where $C^2 = \sum_j b_{ij}^2/16$. A more formal derivation of formula (10) is given in the Appendix.

Series (9) is easily summed with the use of the Laplace transformation. Thus, for the Laplace transform of the function $G_p(N\tau)$ we obtain

$$L_G(s) = \frac{\omega_c w(s)}{1-\omega_c w(s)}, \quad (11)$$

where $\omega_c = C\sqrt{2}$ and $w(x)$ is the Laplace transform of the Gaussian function—the probability integral of a complex argument, which is tabulated in the book [25]. The behavior of the function $G_p(N\tau)$ at large times, which we are interested in, is defined by the nearest root of the denominator in (11). Thus, an equation for the sought singular point of expression (11) is given by

$$\sqrt{\pi} y \operatorname{erfc}(x)\exp(x^2) = 1, \quad (12)$$

where

$$x = \frac{s}{\sqrt{2M_{2c}(p)}},$$

$$y = \frac{\omega_c(1-p)}{\sqrt{2M_{2c}(p)}} = \left[\frac{5}{4}\left(1+2.4\frac{p^2}{(1-p)^2}\right)\right]^{-1/2}.$$

When $p = 0$, as before [16], an approximate solution to Eq. (12) is given by

$$x_{\min}(0) = 0.47, \quad s_{\min}(0) = 0.47\sqrt{2M_{2c}(0)}, \quad (13)$$

for the propagator $G_0(N\tau)$ and the second moment of the intensity profile, we obtain [16]

$$G_0(N\tau) \approx \exp(0.743CN\tau), \quad K(N\tau) \approx \exp[a(0)N\tau] = \exp(1.486CN\tau). \quad (14)$$

respectively. Note that the values of τ_0 and τ differed little in the experiments of [14] (see Hamiltonian (4)). For instance, the maximum value of the parameter p in [14] was 0.1. Let us evaluate the sought parameters for this value. Now the approximate solution to Eq. (12) yields

$$x_{\min}(0.1) = 0.45, \quad s_{\min}(0.1) = 0.45\sqrt{2M_{2c}(0.1)}.$$

Next, for the exponent

$$K(N\tau) = G_p(N\tau)G(N\tau_0) \approx \exp[a(p)N\tau], \quad (15)$$

which describes the increase in the second moment with time, we will use the estimate

$$a(p) \approx \frac{1}{2}(1-p)x_{\min}(0)\sqrt{2M_{2c}(0)} + \frac{1}{2}x_{\min}(p)\sqrt{2M_{2c}(p)}.$$

For small values of p, we can neglect the shift of $x_{\min}(p)$ and the contribution of H_d to $M_{2c}(p)$ and use the expression

$$a(p) \approx a(0)(1-p). \quad (16)$$

The Gaussian function $\exp(-A^2M^2t^2)$ in (7), which describes the decay of an MQ coherence as a function of the order M, was obtained in [23] in the adiabatic approximation under the condition that each spin in the lattice is surrounded by a large number of approximately equivalent neighbors. The exponent of this function was obtained as a sum of a large number of independent contributions of each neighbor of fixed spin to the variation of its phase averaged over the positions of spins in the lattice (see the Appendix in [23]). The quantity A^2, which ultimately turns into a parameter, was initially formed as [23]

$$A^2M^2\frac{t^2}{2} \approx M^2\frac{t^2}{2}\sum_j\left(\frac{1}{K}\sum_{i=1}^{K} b_{ij}\right)^2, \quad (17)$$

where the indices i and j number all the spins that belong and do not belong to the given cluster, respectively; t is the action time of the Hamiltonian H_d on MQ coherences prepared during time $N_0\tau_0$ (here N_0 is the number of cycles; Fig. 1a); and K' is the total number of spin-raising and spin-lowering operators defined on the cluster. To facilitate the comparison of the theory with experimental results, it is expedient to pass to new time variables that allow one to directly take into account a multiple (N-fold) repetition of the experimental cycle (see Fig. 1). Therefore, we set

$$T_0 = N_0\tau_0, \quad T = N\tau.$$

In the case of simultaneous emergence and degradation of MQ coherences (see Fig. 1b), a coherence that arises at time instant t under the interaction $(1-p)H_0$ from Hamiltonian (4) on the time interval $[0, T]$ will further degrade under the interaction pH_d from Hamiltonian (4); the decay occurs during a time interval of $T-t$. It follows from the aforesaid that, to describe the degradation in the experiment (Fig. 1b), one should replace time t in (17) by $\langle T-t\rangle$. Here the symbol $\langle\ldots\rangle$ denotes averaging with respect to the emergence instant of a coherence. Thus, for a function

describing the decay of a coherence with a given M, we obtain

$$\Gamma_M(t) \propto \exp[-p^2A^2M^2\langle(T-t)^2\rangle]. \quad (18)$$

To perform the averaging in (18), we should find $R(t)$, the probability density of emerging a coherence as a function of time. This can be done in the general form both for the experiment illustrated by the scheme in Fig. 1b and for the experiment with the scheme in Fig. 1c. According to the results of [10, 11, 16], the average number of coherences grows exponentially with time (henceforth, we will assume for short that $a(0) = a_0$ and $a(p) = a_p$:

$$K(t) = \begin{cases} \exp(a_0 t), & 0 < t < T_0 \\ \exp(a_0 T_0)\exp[a_p(t-T_0)], & T_0 < t < T + T_0. \end{cases} \quad (19)$$

Formula (19) shows that the exponent characterizing the growth rate of the number of correlated spins is different from that in the classical situation [10, 11, 16]. The sought probability density is determined by the time derivative [26] of expression (19):

$$R(t) = \frac{1}{D}\frac{dK(t)}{dt}, \quad (20)$$

where D is a normalization constant,

$$D = \exp(a_0T_0 + a_pT) - 1. \quad (21)$$

Now we can obtain the time average in (18):

$$\langle(t-(T_0+T))^2\rangle = T^2\int_0^{T_0} R(t)dt + \int_{T_0}^{T_0+T} R(t)[t-(T_0+T)]^2dt. \quad (22)$$

Note that the coherences that appeared in the interval $[0, T_0]$ relax during the entire interval $[T_0, T_0 + T]$ (see Fig. 1c) and make a contribution proportional to T^2 to (22). Performing the integration and taking into consideration relations (19)–(21), we finally obtain

$$\langle(t-(T_0+T))^2\rangle = \frac{2}{a_p^2D}\exp(a_0T_0 + a_pT) - \frac{2}{a_pD}\left(T + \frac{1}{a_p}\right)\exp(a_0T_0) - \frac{T^2}{D}. \quad (23)$$

Substituting (23) into formula (18), we find the sought result for the time correlation function describing the relaxation of coherence amplitudes of different orders in the MQ spectrum and, hence, for the effective mean size of a cluster K_{eff} observed in the experiments in [14]. Hence, to describe the experiments of [14], one should apply the expression

$$K_{\text{eff}}(T_0, T) = [(K(T_0+T))^{-1} + A^2p^2\langle(t-(T_0+T))^2\rangle]^{-1} = \left[\exp(-a_0T_0 - a_pT) + A^2p^2 \times \left\{\frac{2}{a_p^2D}\exp(a_0T_0 + a_pT) - \frac{2}{a_pD}\left(T + \frac{1}{a_p}\right)\exp(a_0T_0) - \frac{T^2}{D}\right\}\right]^{-1} \quad (24)$$

instead of formula (8). Since formulas (23) and (24) are rather cumbersome, it is worthwhile to consider some limit cases for the relation between the parameters.

1. Let $T = 0$. Then $\langle(t-T_0)^2\rangle = 0$ and hence

$$K_{\text{eff}} = K(T_0) = K_0.$$

2. Let $a_pT \ll 1$. Then

$$\langle(t-(T_0+T))^2\rangle \approx \begin{cases} T^2(1 + a_pT/3), & a_0T_0 \gg 1, \\ T^2\dfrac{a_0T_0 + a_pT/3}{a_0T_0 + a_pT}, & a_0T_0 \ll 1 \end{cases} \quad (25)$$

and

$$K_{\text{eff}} \approx \begin{cases} \dfrac{K(T_0+T)}{1 + A^2p^2T^2K(T_0+T)}, & a_0T_0 \gg 1, \\ \dfrac{K(T_0+T)}{1 + A^2p^2T^2K(T_0+T)/3}, & a_0T_0 \ll 1. \end{cases} \quad (26)$$

3. Let $a_pT \gg 1$. Then $\langle(t-(T_0+T))^2\rangle \approx 2/a_p^2$ and

$$K_{\text{eff}} \approx \frac{K(T_0+T)}{1 + 2K(T_0+T)A^2p^2/a_p^2}.$$

For $2K(T_0 + T)A^2p^2/a_p^2 \gg 1$, K_{eff} reaches its steady state given by

$$K_{\text{eff}} \approx \frac{a_p^2}{2A^2p^2}. \quad (27)$$

Note that, for the experimental scheme illustrated in Fig. 1b, one should set $T_0 = 0$ in formulas (24)–(27).

The functions $K_{\text{eff}}(T)$ calculated for various values of the parameters by formula (24) are shown in Fig. 2 (the experimental scheme of Fig. 1b) and Fig. 3 (the experimental scheme of Fig. 1c).

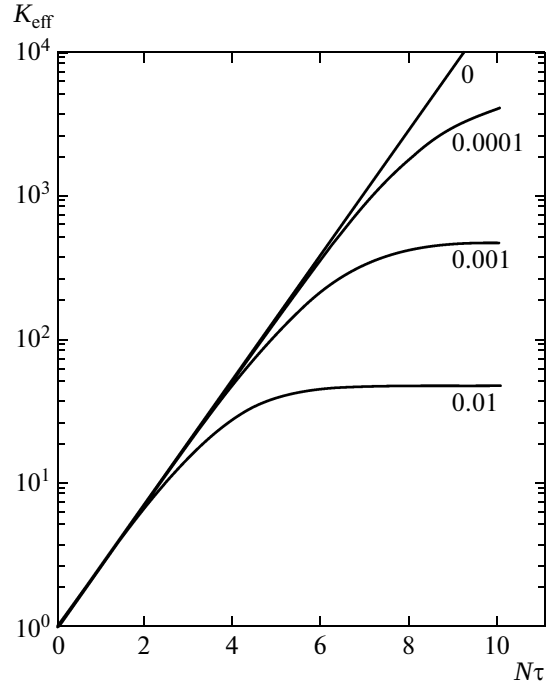

Fig. 2. Evolution of the effective size of a cluster under conditions of Fig. 1b for various values of the parameter A^2p^2/a_p^2 (the numbers under appropriate curves). Time is given in the units of $1/a_0$.

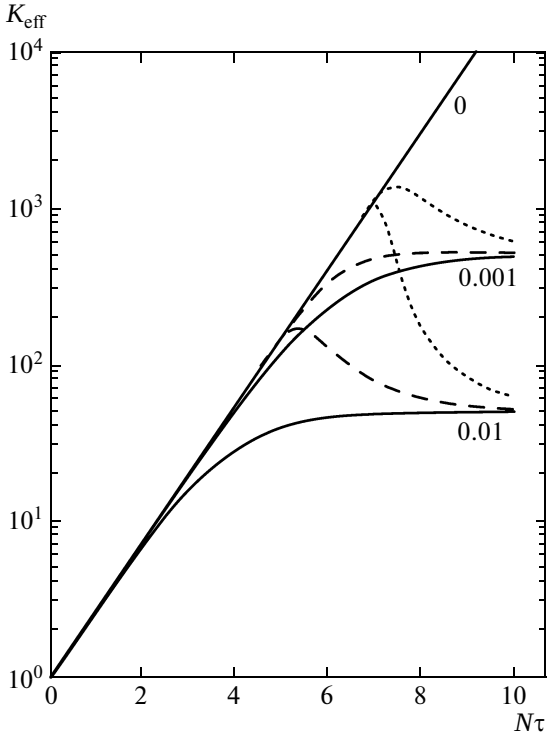

Fig. 3. Evolution of the effective size of a cluster according to the scheme of Fig. 1c under different initial conditions: $T_0a_0 = 0$ (solid lines), $T_0a_0 = 5$ (dashed lines), and $T_0a_0 = 7$ (dotted lines). The numbers at the curves indicate the values of the parameter A^2p^2/a_p^2 (time is given in the units of $1/a_0$).

5. DISCUSSION OF THE RESULTS

The time dependence of the effective number K_{eff} of correlated spins illustrated in Figs. 2 and 3 shows good agreement with the experimental results of [14] and adequately reflects all the characteristic features in the behavior of the experimental functions. We should put special emphasis on the most important result of the theory presented—the fact that the effective cluster size K_{eff} reaches a steady-state value predicted by (27). Such a stabilization of the cluster size was indeed observed in [14] (see Fig. 5 in [14]); just as in (27), the experimental effective cluster size was inversely proportional to the square of the parameter p (formula (5)). The experimental value of the coefficient multiplying this function did not quite coincide with the earlier determined ratio $a_p^2/2A^2$ of earlier defined constants [16, 23]. This is likely to be attributed to the mutual effect of two terms in Hamiltonian (4), which acted separately under the conditions of the previous experiments considered in [16, 23].

According to the aforesaid, this stabilization of the cluster size is associated with the behavior of the MQ coherence profile as a function of the order M. Indeed, the dependence of the MQ spectrum on M is expressed as

$$g_M(T_0, T) \propto \exp\left[-\frac{M^2}{K(T_0 + T)}\right] \times \exp[-A^2M^2p^2\langle(t-(T_0+T))^2\rangle]. \quad (28)$$

The number K in (28) grows exponentially with T; therefore, the dependence on M of the first cofactor becomes weaker, and the dependence of the MQ spectrum on M is completely determined by the second cofactor in (28), where, according to (27),

$$\langle\Delta t^2\rangle = \langle(t-(T_0+T))^2\rangle \approx 2/a_p^2.$$

This result is attributed to the fact that the maximum number of coherences arises near the boundary $t = T_0 + T$. At a distance of Δt away from this boundary toward smaller times, the number of emerging coherences decays exponentially (as $\exp(-a_p\Delta t)$). The mean value of the time variable $\langle\Delta t^2\rangle$ in (22) is bounded by this exponential function and equals $2/a_p^2$; therefore, the exponent of the second cofactor in (28) becomes independent of T_0 and T:

$$g_M \propto \exp(-2A^2M^2p^2/a_p^2). \quad (29)$$

Thus, the intensity profile becomes time-independent; therefore, the mean cluster size defined by the half-maximum bandwidth also becomes independent of T_0 and T, whereas a real cluster continues to grow.

In the recent publication [27],[1] the authors of [14] argue that the distribution of coherences of different orders in the MQ spectrum is described by the exponential function

$$g_M(N_0\tau_0) \propto \exp[-|M|/\sqrt{K(N_0\tau_0)}] \tag{30}$$

rather than by the Gaussian function. Although the first cofactor in (28) in this case is changed, this does not significantly influence the calculations that lead to formula (29). Now the transition from (28) to (29) with increasing time is not described in detail by the simple formula (24). To obtain the function $K_{\text{eff}}(T)$ under new conditions, one should solve the system of two equations

$$\begin{aligned} &\frac{|M|}{\sqrt{K_{\text{eff}}(T_0+T)}} = 1, \\ &\frac{|M|}{\sqrt{K(T_0+T)}} + p^2A^2M^2\langle(t-(T_0+T))^2\rangle = 1. \end{aligned} \tag{31}$$

We should specially stress that the choice of one or other shape function of the MQ spectrum for describing the results of the experiments of [14, 27] or for the numerical simulation [7, 17] is not unique until we construct a rigorous microscopic theory and carry out experiments with low error for the required results.

Let us point out that, in the definition of K_{eff} by (30), (31), its steady-state value (27) is preserved even under the variation of the shape of the MQ spectrum and the decay of MQ components as a function of M in rather wide limits, because the decay is completely determined by the steady-state value

$$\langle\Delta t^2\rangle = \langle(t-(T_0+T))^2\rangle \approx 2/a_p^2.$$

In turn, the steady-state value of averaged time is determined by the fast exponential growth (19) of the mean cluster size, which is characterized by the second moment of the MQ spectrum (15) rather than by the shape of this spectrum.

APPENDIX

In this Appendix, we derive formula (10). Following [16], we write

$$M_{2c}(p) = \frac{1}{2}M_{2c}^{(1)}(p) + \frac{1}{2}M_{2c}^{(2)}(p), \tag{A.1}$$

where $M_{2c}^{(1)}(p)$ is the second moment per one link of the simplest chain and $M_{2c}^{(2)}(p)$ is the second moment per one link for a chain with the maximum number of simplest regions.

[1] An addition made after referee's corrections.

1. In the simplest chain, regions with spin projections x and y successively alternate on the diagram; these regions correspond to autocorrelation functions $\Gamma_x(t)$ and $\Gamma_y(t)$ with equal second moments,

$$\begin{aligned} M_{2c}^{(1)}(p) = M_{2x} = M_{2y} &= -\frac{\text{Tr}([H_{\text{eff}}, S_{yi}])}{\text{Sp}S_{yi}^2} \\ &= (1-p^2)C^2 + p^2B^2, \end{aligned} \tag{A.2}$$

where

$$C^2 = \frac{1}{16}\sum_j b_{ij}^2, \quad B^2 = \sum_j b_{ij}^2 = 4C^2.$$

2. In the chain with the maximum number of simplest regions, regions with spin projections z and y successively alternate on the diagram. For the second moment of the autocorrelation functions $\Gamma_z(t)$, we obtain

$$M_{2z} = -\frac{\text{Tr}([H_{\text{eff}}, S_{zi}]^2)}{\text{Sp}S_{zi}^2} = 2(1-p)^2C^2. \tag{A.3}$$

Hence,

$$\begin{aligned} M_{2c}^{(2)}(p) &= \frac{1}{2}M_{2z} + \frac{1}{2}M_{2y} \\ &= \frac{3}{2}(1-p)^2C^2 + \frac{1}{2}p^2B^2. \end{aligned} \tag{A.4}$$

Substituting (A2) and (A4) into (A1), we obtain the required result (10).

Notice that formulas (A2) and (A3) are obtained in the approximation of zz interaction for H_d, i.e., under the assumption that the interaction between the spin components S_{zi} are preserved in the Hamiltonian H_d, while the interactions with the spin components S_{xi} and S_{yi} are dropped out. Under the total Hamiltonian H_d, the terms $\frac{1}{4}B^2p^2$ and $\frac{1}{2}B^2p^2$ are added to the second moments M_{2y} and M_{2z}, respectively. Finally, the notations of spin components here and in paper [16] are related by cyclic permutations.

REFERENCES

1. R. Ernst, G. Bodenhausen, and A. Wokaun, *Principles of Nuclear Magnetic Resonance in One and Two Dimensions* (Clarendon, Oxford, 1987; Mir, Moscow, 1990).
2. M. Munovitz and A. Pines, Adv. Chem. Phys. **6**, 1 (1987).
3. J. Baum, M. Munovitz, A. N. Garroway, and A. Pines, J. Chem. Phys. **83**, 2015 (1985).
4. V. L. Bodneva and A. A. Lundin, JETP **108** (6), 992 (2009).
5. P.-K. Wang, J.-P. Ansermet, S. L. Rudaz, Z. Wang, S. Shore, C. P. Slichter, and J. H. Sinfelt, Science (Washington) **234**, 35 (1986).
6. J. Baum and A. Pines, J. Am. Chem. Soc. **108**, 7447 (1986).

7. S. I. Doronin, A. V. Fedorova, E. B. Fel'dman, and A. I. Zenchuk, J. Chem. Phys. **131**, 104109 (2009).
8. R. H. Schneder and H. Schmiedel, Phys. Lett. A **30**, 298 (1969).
9. W. K. Rhim, A. Pines, and J. S. Waugh, Phys. Rev. B: Solid State **3**, 684 (1971).
10. H. G. Krojanski and D. Suter, Phys. Rev. Lett. **93**, 090501 (2004).
11. H. G. Krojanski and D. Suter, Phys. Rev. Lett. **97**, 150503 (2006).
12. H. G. Krojanski and D. Suter, Phys. Rev. A: At., Mol., Opt. Phys. **74**, 062319 (2006).
13. M. S. Lovric, H. G. Krojanski, and D. Suter, Phys. Rev. A: At., Mol., Opt. Phys. **75**, 042305 (2007).
14. G. A. Alvarez and D. Suter, Phys. Rev. Lett. **104**, 230403 (2010).
15. G. Cho, P. Capprlaro, D. G. Cory, and C. Ramanathan, Phys. Rev. B: Condens. Matter **74**, 224434 (2006).
16. V. E. Zobov and A. A. Lundin, JETP **103** (6), 904 (2006).
17. S. I. Doronin, E. B. Fel'dman, and F. I. Zenchuk, J. Chem. Phys. **134**, 034102 (2011).
18. R. Balesçu, *Equilibrium and Non-Equilibrium Statistical Mechanics* (Wiley, New York, 1975; Mir, Moscow, 1978), Vol. 2.
19. W. H. Zurek, Rev. Mod. Phys. **75**, 715 (2003).
20. P. W. Anderson, *Basic Notions of Condensed Matter Physics* (Benjamin/Cummings, San Francisco, California, United States, 1984).
21. P. W. Anderson and P. R. Weiss, Rev. Mod. Phys. **25**, 269 (1953).
22. A. Abragam, *Principles of Nuclear Magnetism* (Oxford University Press, Oxford, 1961; Inostrannnaya Literatura, Moscow, 1963), Chap. 4.
23. V. E. Zobov and A. A. Lundin, JETP **112** (3), 451 (2011).
24. U. Haeberlen and M. Mehring, *High Resolution NMR Spectroscopy in Solids* (Springer, New York, 1976; Mir, Moscow, 1980).
25. *Handbook of Mathematical Functions: With Formulas, Graphs, and Mathematical Tables*, Ed. by M. Abramowitz and I. Stegun (Dover, New York, 1965 Nauka, Moscow, 1979).
26. B. V. Gnedenko, *Theory of Probability* (Nauka, Moscow, 1988; Gordon and Breach, Amsterdam, 1997).
27. G. A. Alvarez and D. Suter, arXiv:1103.4546 [quant-ph].

Translated by I. Nikitin